Astron. Astrophys. 332, 46–54 (1998)

ASTRONOMY
AND
ASTROPHYSICS

IR spectra of young Magellanic Cloud clusters and starburst galaxies: constraints on the temperature of red supergiants and new estimates of metallicity in young stellar populations⋆

E. Oliva[1] **and L. Origlia**[2]

[1] Osservatorio Astrofisico di Arcetri, Largo E. Fermi 5, I-50125 Firenze, Italy
[2] Osservatorio Astronomico di Bologna, Via Zamboni 33, I-40126 Bologna, Italy

Received 28 May 1997 / Accepted 5 December 1997

Abstract. Infrared spectra of young stellar clusters in the Magellanic Clouds are used to derive information on the red supergiants dominating their 1.6 μm emission, and to obtain a new and independent estimate of their metallicities. The most striking result is that red supergiants with low metallicity appear to be much cooler than predicted by evolutionary models, and this most probably reflects uncertainties in the calibration of the mixing–length parameter in the outermost layers of the stellar envelopes. The metallicity [Fe/H] can be estimated from the $W_\lambda(1.62)$ index which is here calibrated using synthetic stellar spectra, and the new scale is also applied to eight starburst galaxies. The resulting values of [Fe/H] range between –1.3 for the SMC cluster NGC330 (in excellent agreement with previous estimates) to –0.2 for the LMC cluster NGC1994. Starburst galaxies have metallicities ranging between –1.0 (NGC6240) and –0.5 (NGC7552). The spectra are also used to estimate the Carbon depletion which in MC clusters is found compatible with a 'standard' value of [C/Fe]$\simeq$–0.3. Interestingly, our spectra show possible evidence of significant variations of Carbon depletion in some starburst galaxies. Finally, the Silicon relative abundance is estimated from the $W_\lambda(1.59)$ index. In MC clusters we find [Si/Fe]$\approx$+0.5, i.e. values similar to those of old clusters in our galaxy and compatible with primordial Si–enhancement by type II supernovae.

Key words: galaxies: abundances – Magellanic Clouds – galaxies: starbust – galaxies: star clusters – supergiants – infrared: stars

1. Introduction

In order to date the star formation events and estimate the metal content of stellar clusters and galaxies one should define and calibrate observable quantities which trace the most luminous stellar population and which could be used to disentangle age and metallicity. In the last years different spectral and population synthesis techniques have been used by many authors (see e.g. Worthey 1994 and references therein) and a number of different age and/or metallicity indicators have been proposed.

A major problem in defining *ideal* stellar tracers is to find suitable integrated quantities which can be easily measured in stars, stellar clusters and galaxies, and which are mainly sensitive to specific stellar parameters. Unfortunately, colors are equally sensitive to age and metallicity, and there is no simple way to disentangle the two effects when studying integrated stellar populations. Spectroscopic indices have the advantage of being more directly dependent on metallicity, and are basically independent on reddening. In complex objects such as active galaxies, spectroscopic indices could also provide a powerful tool to isolate the stellar contribution from other continuum sources. In Origlia et al. (1993, hereafter OMO93, and 1997, hereafter OFFPO97) and in Oliva et al. (1995, hereafter OOKM95) we showed how near IR spectroscopic indices could be used for this purpose. Specific advantages of working around 1.6 μm are low extinction, small contamination by non-stellar continuum sources and the fact that the near IR stellar luminosity is dominated by a quite homogeneous stellar population of red giants and/or supergiants whose properties are quite sensitive to age and metallicity (e.g. Renzini and Buzzoni 1986, Chiosi et al. 1986), and their spectra contain many strong IR absorption features due to neutral metals and molecular species (OMO93) which are also present in the spectra of all types of galaxies (OOKM95).

In OMO93 we selected 3 absorption features at 1.59 μm (Si + OH), at 1.62 μm [dominated by the CO(6,3) band-head] and 2.29 μm [CO(2,0) band-head] which are prominent and relatively easy to measure in the IR spectra of stars and galaxies. The variation of these indices with stellar parameters was investigated in much details and the CO 1.62 μm index was used to derive a metallicity scale for old stellar populations. This was successfully applied to well known globular clusters

Send offprint requests to: E. Oliva

⋆ Based on observations collected at the European Southern Observatory, La Silla, Chile

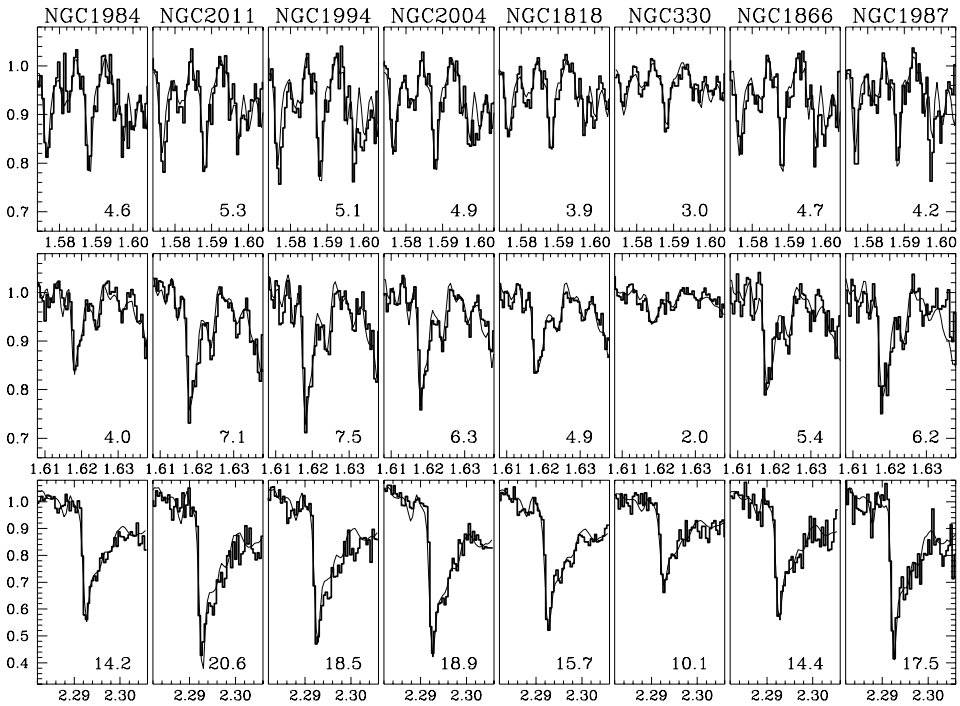

Fig. 1. Normalized IRSPEC spectra of young Magellanic Cloud clusters centered at 1.59 μm (Si+OH), 1.62 μm [CO(6,3) band-head] and 2.29 μm [CO(2,0) band-head]. Wavelengths (μm) are in the rest frame. The thin lines show the result of the spectral fitting used to normalize the spectra and to derive the feature equivalent widths (in Å, given at the bottom right of each panel). See Sect. 2 and OOKM95 for details.

and normal galaxies (OFFPO97). The equivalent width of the 1.59 μm index was found to primarily, though slowly depend on the [Si/H] abundance, and the estimated [Si/Fe] abundance anomalies were $\approx$+0.5 dex and compatible with current ideas on the enhancement of α elements. Finally, the CO 2.29 μm index was found to be a useful tool to estimate the atmospheric microturbulent velocity.

In this paper we present a similar analysis and investigate the possible use of the IR indices to study the properties of red supergiants in young clusters, and to estimate their metallicities. As observational templates we use young stellar clusters in the Magellanic Clouds (MC) and well studied starburst galaxies.

The paper is organized as follows. The observations are presented in Sect. 2 while Sect. 3 discusses the physical parameters of red supergiants and their influence on the IR spectral indices. The new metallicity scale is derived and applied in Sect. 4 while atmospheric microturbulent velocities are derived and discussed in Sect. 5. The effect of Carbon depletion is analyzed in Sect. 6 while the relatively weak constraints on the Silicon abundance are discussed in Sect. 7. Finally, in Sect. 8 we draw our conclusions.

2. Observations and data reduction

The data were collected during several observing runs between 1991 and 1993 at the ESO-NTT telescope using the IRSPEC infrared spectrometer (Moorwood et al. 1991, Gredel & Weilenman 1992) equipped with a SBRC 62x58 InSb array detector. The pixel size was 2.2 arcsec along the slit and $\simeq$5 Å along the dispersion direction which with a 2 pixels (4.4") slit yielded a resolving power $R \simeq$1600 and 2500 at 1.6 and 2.3 μm, respectively.

For each cluster we obtained three spectra centered at 1.59, 1.62 and 2.29 μm to include the absorption stellar features of interest. Each spectrum consisted of several ABBA cycles (A–object in the slit, B–sky a few arc-minutes out of the cluster center) and each exposure was the mean of two 60 second frames. The total integration time per spectrum varied from 10 to 40 minutes depending on the brightness of the cluster. Data reduction was performed using the IRSPEC context of MIDAS. The 2D spectra were sky subtracted and flat field corrected using measurements on an halogen lamp. The 1D spectra were obtained extracting and adding the central rows (4.4"x11" field of view) and were spectroscopically calibrated (i.e. corrected for instrumental + atmospheric transmission) using spectra of O5/O6 stars taken at the same grating positions as the object. More details about data reduction can be found in Oliva & Origlia (1992), OMO93, OOKM95 and in the MIDAS manual.

The spectra were normalized using the fitting procedure described in Sect. 2.1 of OOKM95. In short, this uses a grid of template stellar spectra taken with the same instrument and best fits the observed data also allowing for line broadening, this last effect was however found to be unimportant for LMC clusters (i.e. all observed features are basically unresolved). The equivalent widths result directly from the fitting procedure, and are measured on the wavelength ranges defined at page 540 of OMO93.

The normalized spectra of the eight MC clusters (7 in the Large and 1 in the Small Magellanic Cloud) are displayed in Fig. 1 together with the fitted profiles and the derived equivalent widths which are also listed in Table 1. Typical accuracies for W_λ(1.59), W_λ(1.62) are $\pm$0.5 Å while W_λ(2.29) is $\pm$1 Å. Table 1 also lists cluster parameters from the literature, namely the metallicity (Sagar & Pandey 1989, note that the values are

Table 1. Observed equivalent widths and derived quantities

Object[(1)]	s[(2)]	$\log t$[(2)]	$[Fe/H]^{(3)}_{Lit}$ (dex)	$[Fe/H]^{(4)}_{1.62}$ (dex)	$W_\lambda(1.59)$[(5)] (Å)	$W_\lambda(1.62)$[(5)] (Å)	$W_\lambda(2.29)$[(5)] (Å)	ξ[(6)] (km/s)	[Si/Fe][(7)] (dex)
MC Clusters									
NGC1984	11	6.9	–	–0.90	4.6	4.0	14.2	3.4	+0.6
NGC2011	13	7.1	–	–0.47	5.3	7.1	20.6	6.1	+0.4
NGC1994	15	7.2	–	–0.24	5.1	7.5	18.5	4.5	+0.4
NGC2004	15	7.2	–	–0.55	4.9	6.3	18.9	5.2	+0.4
NGC1818	18	7.5	–1.6,–0.9[b]	–0.74	3.9	4.9	15.7[c]	3.9	+0.4
NGC330	19	7.6	–1.8,–1.3	–1.33	3.0	2.0	10.1	2.3	+0.5
NGC1866	27	8.2	–1.2,–0.1	–0.55	4.7	5.4	14.4	3.1	+0.6
NGC1987	35	8.8	–	–0.50	4.2	6.2	17.5	4.4	+0.3
Starbursters[a]									
NGC253	–	–	–	–0.66	3.9	4.9	14.0	3.0	+0.4
NGC1614	–	–	–	–0.73	3.8	5.1	16.6	4.3	+0.3
NGC1808	–	–	–	–0.66	4.0	5.1	15.0	3.4	+0.4
NGC3256	–	–	–	–0.56	3.9	5.1	12.9	2.5	+0.4
NGC4945	–	–	–	–0.79	3.9	4.8	16.4	4.3	+0.3
NGC6240	–	–	–	–1.00	3.3	4.2	17.8	5.7	+0.2
NGC7552	–	–	–	–0.54	3.4	5.2	14.2	3.0	+0.2
NGC7714	–	–	–	–0.56	3.5	5.1	13.9	2.9	+0.3

Notes to Table 1
(1) Clusters in the Magellanic clouds are ordered by increasing age
(2) 's' is the age parameter, cluster age (yr) is $\log t \sim 0.079s + 6.05$ (Elson & Fall 1985, 1988)
(3) Values of metallicity from the compilation by Sagar & Pandey (1989)
(4) New estimate of [Fe/H] based on the $W_\lambda(1.62)$ index (Eqs. 1,2) and assuming [C/Fe]=–0.3, typical errors are $\pm$0.4 dex
(5) Measured equivalent width. Each absorption feature is integrated on a specific wavelength range which is defined at page 540 of OMO93
(6) Microturbulent velocity derived from $W_\lambda(1.62)$ and $W_\lambda(2.29)$ (Fig. 5 and Eq. 2), typical errors are $\pm$1 km/s.
(7) Silicon relative abundance necessary to obtain the observed $W_\lambda(1.59)$ once the $[Fe/H]_{1.62}$ is adopted, typical errors are $\pm$0.6 dex
[a] Data for starbursters are from OOKM95 except for NGC6240 which is based on IRSPEC spectra to appear in a forthcoming paper
[b] Higher metallicity from Meliani (1994)
[c] The value of $W_\lambda(2.29)$ for NGC1818 was incorrectly reported in Table 2 of OOKM95

quite uncertain for most clusters) and the s–parameter which is related to the cluster ages

$$\log t \simeq 0.079s + 6.05 \qquad \text{yr}$$

(Elson & Fall 1985, 1988) which are also listed in Table 1. It should be noted however that the s–age relationship may suffer by important uncertainties depending on the assumed calibration scale (e.g. Ferraro et al. 1995 and references therein).

3. Physical parameters of red supergiants

3.1. IR spectral indices and stellar parameters

To calibrate the variation of IR indices with metallicity and other stellar parameters we used the grid of synthetic stellar spectra described in OFFPO97 which was here extended to larger microturbulent velocities to properly sample the parameters of the very luminous red supergiants which dominate the IR emission of the young MC clusters.

The behaviour of the IR indices in synthetic spectra can be visualized in Fig. 2 which plots their variation with metallicity for a few representative combinations of stellar parameters. This is equivalent of Fig. 1 of OFFPO97 but for cooler temperatures, larger microturbulent velocities and lower gravities. The main characteristics outlined by OFFPO97 are still valid in the selected range of parameters more suitable for young stellar populations. The 1.62 index is a complex function of Carbon abundance, surface gravity, temperature and, to a lesser extent, microturbulent velocity. The 2.29 index is mainly sensitive to the microturbulent velocity ξ, while the 1.59 index is basically independent on all parameters but the Si abundance.

3.2. Evolutionary tracks and the variation of stellar parameters with metallicity and age

A proper calibration of the IR indices with metallicity and age requires adopting a relationship between stellar parameters (temperature, gravity, ξ), age and metallicity. For old stellar populations both T_{eff} and $\log g$ are relatively well defined at a given

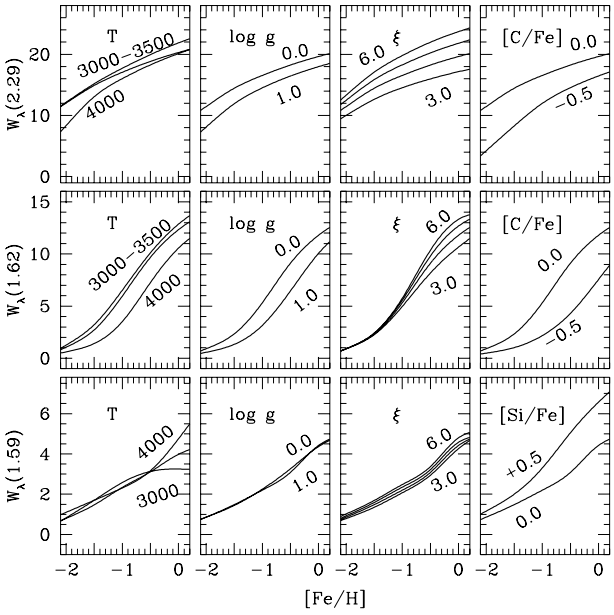

Fig. 2. Variation with metallicity of the equivalent widths (in Å) of the IR absorption features as predicted by synthetic stellar spectra. The parameters of the reference model are T_{eff}=3600 K, log g=0.0, ξ=4 km/s and solar relative abundances of metals, i.e. [C/Fe]=0.0 and [Si/Fe]=0.0. Each panel shows the effects of varying effective temperature T_{eff}, surface gravity log g, microturbulent velocity ξ and abundance anomalies [C/Fe], [Si/Fe].

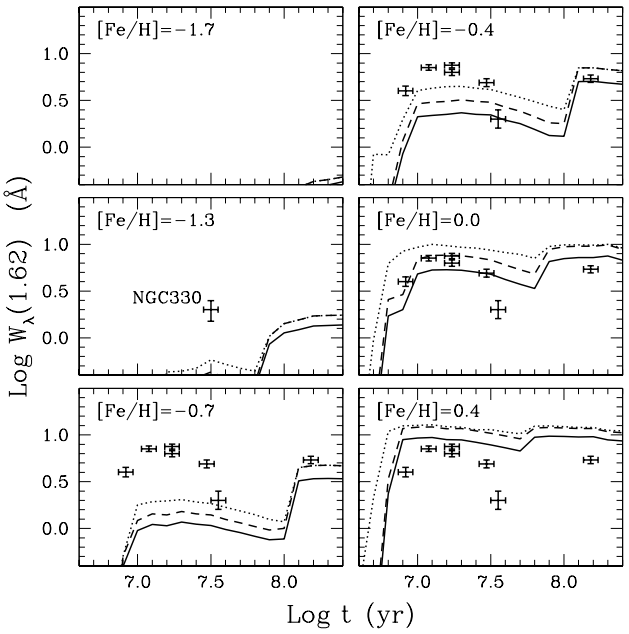

Fig. 3. Predicted variation of $W_\lambda(1.62)$ with age at various metallicities adopting the theoretical isochrones of Bertelli et al. (1994). The solid lines are for typical values of Carbon relative abundance, [C/Fe]=–0.3 dex, and microturbulent velocity, ξ=3 km/s, while the dashed curves are for [C/Fe]=0.0, ξ=6 km/s and represent the maximum values of $W_\lambda(1.62)$ compatible with the above mentioned evolutionary models. The dotted curves also assume [C/Fe]=0.0, ξ=6 km/s and show the results of artificially eliminating the 'blue–loops' in the evolution of massive star (see text, Sect. 3.2). The crosses are the data for MC clusters whose ages were estimated from the s-parameter (cf. Sect. 2). Note that the theoretical curves predict very weak $W_\lambda(1.62)$ at low metallicities, but this is not confirmed by our spectra of NGC330, a thoroughly study, low metallicity ([Fe/H]$\lesssim$–1.3) cluster in the SMC. More generally, our spectra indicate that the red supergiants dominating the IR emission of young clusters are much cooler than predicted by current evolutionary tracks (cf. Sect. 3.2 for more details).

metallicity and age, but the situation for young stars is much more uncertain as the post main sequence evolution strongly depends on the assumed input physics.

A simple and instructive exercise is to use published isochrones to predict the strength of the 1.62 index at various ages and metallicities. The integrated value of the spectral index is given by

$$\overline{W_\lambda(1.62)} = \frac{\int \phi(M)\, L_{\rm H}(M)\, W_\lambda(1.62)\{T, g, \xi, [\rm C/Fe]\}\, dM}{\int \phi(M)\, L_{\rm H}(M)\, dM}$$

where T=$T(M)$ and g=$g(M)$ are the stellar temperature and gravity along an isochrone which are predicted by evolutionary models, $L_{\rm H}(M)$ is the predicted stellar luminosity at 1.62 μm and $\phi(M) \propto M^{-2.35}$ is the Salpeter's initial mass function. The values of microturbulent velocity, ξ, and Carbon relative abundance, [C/Fe], along the isochrone cannot be easily predicted and must be therefore treated as free parameters.

The results of this exercise are displayed in Fig. 3 which plots the predicted time variation of the 1.62 index at various metallicities. The most remarkable result is that young ($<10^8$ yr) clusters with metallicities [Fe/H]<–0.7 should have a very weak, and in practice unmeasurable 1.62 μm feature. This derives from the fact that evolutionary tracks predict that red supergiants with low metallicities should be quite warm. Specifically, at $t \simeq 10^{7.5}$ yr and [Fe/H]$\leq$–1.3 (i.e. the age and metallicity of NGC330) the *coolest* stars in the isochrones have T_{eff}>4000 K. At these temperatures the CO/C relative abundance is quite low and the CO features are therefore very shallow.

The predictions of Fig. 3 are in strict contrast with our results on NGC330, an extensively studied SMC cluster whose young age and low metallicity are well established. Taken at face value, the curves in Fig. 3 would imply [Fe/H]$\simeq$–0.4 for NGC330, NGC1866, NGC1987 and embarrassingly large metallicities ($\geq$solar) for the youngest MC clusters of Table 1.

The curves of Fig. 3 are based on the isochrones of Bertelli et al. (1994, hereafter B94) but the main results do not depend on the adopted evolutionary models because, to the best of our knowledge, all theoretical tracks predict similarly high temperatures for red supergiants with low metallicities. Specifically, the evolutionary models of B94, Castellani et al. (1990), Charbonnel et al. (1993) all find that stars with mass larger than 6 $M_\odot$ and [Fe/H]$\leq$–1.0 should never reach effective temperatures T_{eff}<4000 K. This implies that the IR spectra of clusters with age log $t < 7.8$ and metallicity $\leq$–1.0 should have a very

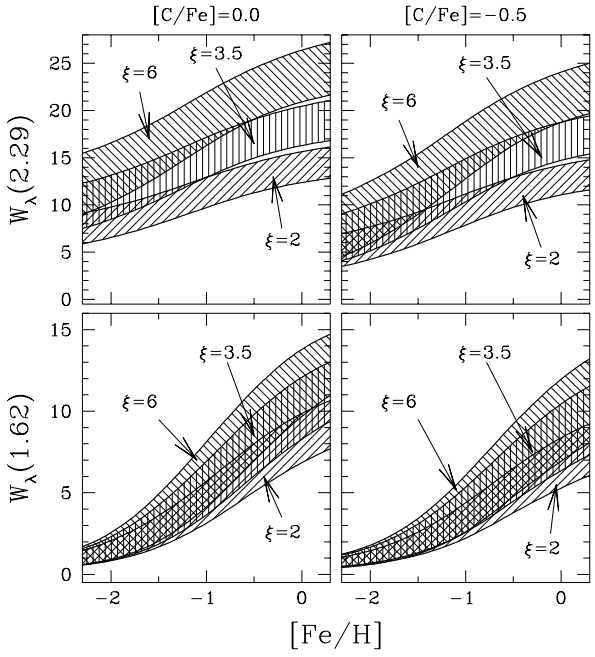

Fig. 4. Predicted variation of the CO–dominated indices as a function of cluster metallicity for solar [C/Fe] (left) and a Carbon depletion of –0.5 dex (right hand panels). At each metallicity a large grid of models with different stellar parameters T_{eff} log g were computed, and the range of equivalent widths obtained is indicated by the shaded areas.

weak CO 1.62 band–head (i.e. $W_\lambda(1.62) \lesssim 0.5$ Å), and this is not confirmed by our spectra.

There are two basic effects which could lead theoretical models to overestimate the temperature of red supergiants.

i) The first and most important is that the temperature of the Hayashi track (i.e. the lowest possible temperature for a red supergiant) is overestimated due to an improper treatment of the opacity and calibration of the mixing–length in the outermost layers of the stellar envelope. This is known to strongly affect the temperature of low mass stars on the red giant branch (Chieffi et al. 1995) but, to the best of our knowledge, no detailed study of its effect on the predicted temperature of red supergiants exists in the literature.

ii) The second possibility is that evolutionary models incorrectly predict that massive stars should spend most of their Helium burning phase at higher temperatures than, and basically never approach the Hayashi track. This effect is evident in the evolution of low metallicity, massive stars (>15 $M_\odot$) which never become red supergiants. However, intermediate mass stars (6–15 $M_\odot$) do approach the Hayashi track, and spend a significant fraction ($\sim$30–50 %) of their He–burning phase as relatively cold red supergiants. The blue–loops to $T_{eff} \lesssim 10^4$ K are relatively unimportant in the tracks of B94[1] have only a minor effect on the IR features, and this is evident in Fig. 3 where we also plot (dotted lines) the results obtained by artificially eliminating the blue–loops from the isochrones. This indicates therefore that the problem discussed here cannot be simply ascribed to the well known uncertainties on the shape and extension of the red–blue loops (e.g. Maeder & Conti 1994, Ritossa 1996).

[1] The blue-loops are much more pronounced in the low–[Fe/H] evolutionary models of the Geneva's group (e.g. Charbonnel et al. 1993), and using these tracks one predicts even weaker CO features (Origlia et al. in preparation).

4. The metallicity scale

Given the uncertainties of the temperatures predicted by theoretical isochrones, we assume for simplicity that the red supergiants dominating the 1.6 μm emission have $T_{eff} \leq 3600$ K, the temperature where most of photospheric Carbon is in the form of CO, and below which the value of $W_\lambda(1.62)$ becomes little dependent on T_{eff}. The lower limit for the temperature is 3000 K but its exact value does not influence the results. The adopted range of surface gravities is $0.0 < \log g < 1.0$.

The predicted variation of the CO indices with metallicity are displayed in Fig. 4 where the shaded areas correspond to the spread of adopted stellar parameters.

An analytical relationship which reproduces the mean variation of $W_\lambda(1.62)$ with [Fe/H] for $T_{eff} \leq 3600$K is

$$[\mathrm{Fe/H}] = \frac{0.3 - 0.10[\mathrm{C/Fe}]}{\xi^{0.3}} \{W_\lambda(1.62) - 2.0\} - 0.8[\mathrm{C/Fe}]$$

$$-0.03\xi - 1.50 \pm 0.3 \quad W_\lambda(1.62) > 2\text{Å} \qquad (1)$$

where the spread of $\pm$0.3 dex corresponds to the width of the shaded areas in Fig. 4.

When compared to the relationship for old stellar populations (Eq. 1 of OFFPO97), the metallicity derived here is less dependent on the value of ξ but is almost directly proportional to the adopted [C/Fe]. This implies that $W_\lambda(1.62)$ is indeed a measurement of the Carbon abundance [C/H], and this is an obvious consequence of the fact that we have not assumed any specific relationship between T_{eff}, log g and [Fe/H]. In old stellar systems we could partially distinguish between [Fe/H] and [C/Fe] (i.e. between total metal abundance and Carbon abundance) because the increase of $W_\lambda(1.62)$ with [Fe/H] is only partially due to the increase of [C/H], but also follows the decrease of T_{eff} and log g with metallicity.

As mentioned above, the choice of the maximum temperature of the red supergiants has strong effects on the results because the fraction CO/C rapidly decreases above 3600 K, and stars with $T_{eff} > 4000$ K have weak CO features even at high metallicities. The global effect of increasing the upper limit in T_{eff} is therefore to extend the lower edges of the shaded areas of Fig. 4, and the metallicity necessary to obtain a given $W_\lambda(1.62)$ roughly increases by +0.3 dex if a temperature range $3600 < T_{eff} < 4000$ is adopted. At higher temperatures the effect is even more dramatic, and assuming $4000 < T_{eff} < 4300$ the derived metallicity must be further increased by $\approx$0.4 dex. In general, values of [Fe/H] from Eq. 1 should be treated as *lower limits* if stars with temperatures >3600 K contribute significantly to the 1.6 μm flux.

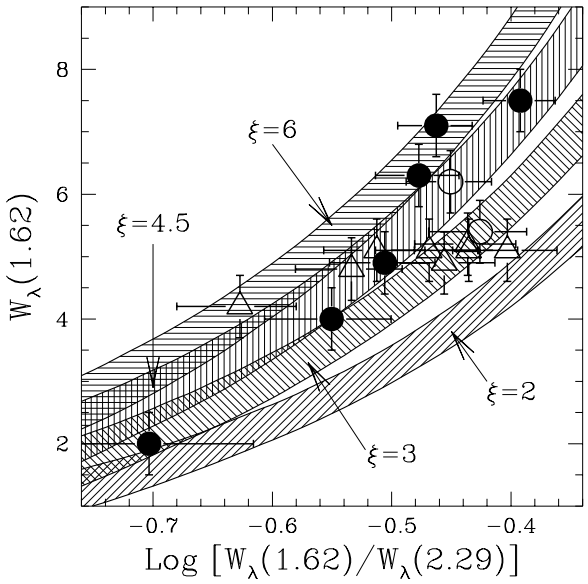

Fig. 5. Observed and predicted behaviour of the CO–dominated indices bands. The data are plotted in the spectroscopic equivalent of a colour–magnitude diagram where the 'magnitude' is $W_\lambda(1.62)$ while the 'colour' is the logarithm of the ratio of the equivalent widths of the 1.62 and 2.29 μm features. Filled circles are clusters with s–parameter $\leq$20, open circles the clusters with $s > 20$ and open triangles the observed starburst galaxies. The shaded areas show the range covered by models with constant microturbulent velocity ξ, the theoretical results can be accurately reproduced by the fitting relationship $y = -0.6 - \xi^{0.96} - 2\xi^{0.8}/(x - 0.07\sqrt{\xi})$ where $y = W_\lambda(1.62)$ and $x = \log[W_\lambda(1.62)/W_\lambda(2.29)]$.

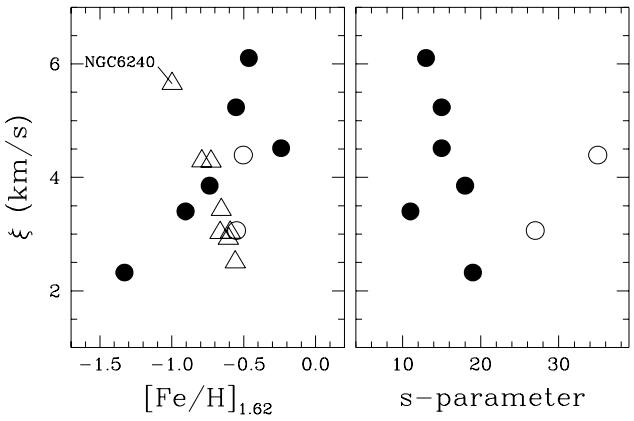

Fig. 6. Variation of microturbulent velocity ξ with metallicity (left) and age parameter (right hand panel). Filled circles are young MC clusters with $s < 20$, open circles are older clusters with $s > 20$ and open triangles are starburst galaxies.

The metallicities listed in Table 1 are from Eq. 1 using the microturbulent velocities derived as described below (Sect. 5) and assuming a 'standard' Carbon depletion of [C/Fe]=–0.3, a value which is also indicated by our spectra (cf. Sect. 6). The quoted uncertainties of $\pm$0.4 dex includes observational errors and the spread of the curves in Figs. 4, 5, but do not include the possible contribution from warmer stars whose net effect would be to increase the derived metallicities to embarrassingly large values (cf. Sect. 3.2). The possible variation of [C/Fe] and its effect on the spectral shape around 1.62 μm is discussed below (Sect. 6).

4.1. Comparison with other metallicity estimates

The inferred metallicities of the MC clusters in our sample ranges between $\sim$1/20 the solar metallicity (NGC330) to about half solar (NGC1994) and are compatible with the few and largely spread estimates available in the literature. The largest discrepancy is for NGC1818 which we find a factor of $\simeq$6 more metallic than the [Fe/H]=–1.6 quoted by Richtler & Nelles (1983), and these authors also derived very low metallicities for NGC1866 and NGC330. However, Meliani et al. (1994) suggested [Fe/H]=–0.9 for NGC1818, while many different authors proposed values in the range –1.8<[Fe/H]<–0.5 for NGC330 (Chiosi et al. 1995 and references therein). Our estimates for NGC330 are within this very broad range and are in good agreement with the values inferred in two red supergiants by Barbuy et al. (1991) and Meliani et al. (1995).

The starburst galaxies in our sample span a relatively narrow range of metallicities, –1.0 to –0.5 dex or equivalently 1/10 to 1/3 solar. These values are systematically lower than those based on O/H abundance estimates in HII regions. For example, Storchi–Bergmann et al. (1994) reported almost solar metallicities for NGC1614, NGC3256 and NGC7714 and about twice solar for NGC7552, while Gonzalez–Delgado et al. (1995) estimated half solar metallicity for NGC7714. These differences may be not significant, taking into account the relatively large uncertainties of our metallicity estimates (cf. Sect. 4) and the intrinsic difficulties of deriving reliable O/H abundances in high metallicity environments (Stasinska & Leitherer 1996 and references therein). On the other hand, these discrepancies seem to be systematic and could also be ascribed to some enhancement of oxygen (an α element) relative to iron, similarly to what found in HII regions (e.g. McGaugh 1991) and in blue compact galaxies (e.g. Marconi et al. 1994)

5. Microturbulent velocities

The microturbulent velocity ξ strongly influences the strength of saturated molecular lines but cannot be easily connected to photospheric temperature, surface gravity or other physical parameters of a given star. However, the value of ξ can be estimated by comparing the strength of the thick CO(2,0) with the thinner CO(6,3) band–heads. The different behaviour of the 1.62 and 2.29 indices with ξ is clearly visible in Fig. 4 but can be best visualized and quantified using a $W_\lambda(1.62)$ vs $W_\lambda(1.62)/W_\lambda(2.29)$ diagram (Fig. 5) where the objects with similar metallicity and temperature but different ξ are displaced horizontally because of their different CO(2,0) strengths. The theoretical curves plotted in Fig. 5 are based on the grid of synthetic stellar models described above.

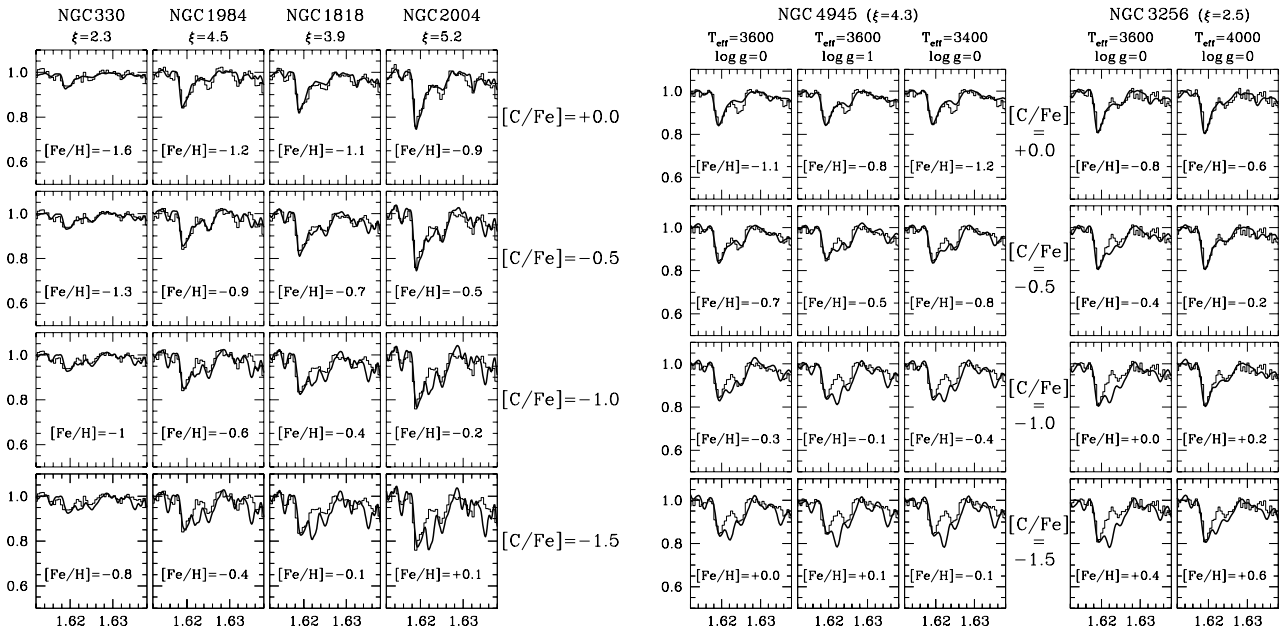

Fig. 7. a Synthetic spectra (thick lines) compared with the observed data (thin histogram) of young Magellanic Cloud clusters. The adopted stellar temperature and gravity are T_{eff}=3600 K and log g=0.0 while the microturbulent velocity is derived from the CO Δv=2 and Δv=3 features (cf. Sect. 5). At each value of Carbon depletion [C/Fe], the metallicity [Fe/H] is chosen to best fit the short wavelength side of the CO(6,3) band-head at 1.619 μm. Note the large predicted strength of OH 1.622, 1625 μm features at [C/Fe]$\lesssim$–1.0. **b** Same as **a** for two starburst galaxies. The synthetic spectra (thick lines) are also computed at different temperatures and gravities to show the effect of these parameters on the relative depths of CO and OH features. The large OH/CO ratio in NGC4945 can be equally well interpreted in terms of unusually large C-depletion, [C/Fe]<–0.5, or with a normal [C/Fe]$\simeq$–0.3 and high surface gravity (second column) or low stellar temperature (third column). Similarly, the weak OH features in NGC3256 could imply almost solar [C/Fe] (fourth column), high stellar temperatures (fifth column) or very low surface gravities. The latter case is not visualized because available model stellar atmospheres do not extend to gravities below log g=0.

The values of ξ can be estimated graphically from Fig. 5 or using the fitting relationship given in the caption which yields

$$\xi = (-y - 0.6)\frac{x - 0.07\xi^{0.5}}{\xi^{-0.04}(x - 0.07\xi^{0.5}) + 2\xi^{-0.2}} \qquad \xi > 2 \quad (2)$$

where y=W_λ(1.62) and x=log[W_λ(1.62)/W_λ(2.29)], the above relationship is the extension to larger ξ of the fitting formula of OFFPO97.

The microturbulent velocities derived from our data are listed in Table 1 (8$^{\rm th}$ column) and plotted in Fig. 6. The values of ξ vary from $\simeq$2 km/s in the lowest metallicity clusters to about 6 km/s in the younger and most metallic objects. The right hand panel of Fig. 6 indicates that the microturbulent velocity is not significantly correlated with age, while a mild correlation between ξ and [Fe/H] for MC clusters is visible in the left panel of Fig. 6. However, starburst galaxies (open triangles) show a much more scattered distribution with the largest microturbulent velocity being associated to the least metallic object (NGC6240) while the most metallic galaxies (NGC3256, NGC7552 and NGC7714) have the lowest ξ's. Although the latter effect could be due to hot dust emission which selectively dilutes the CO(2,0) band–head relative to the 1.62 feature (an effect which often occurs in Seyferts, cf. OOKM95), the uncertainties are however too large to draw any firm conclusion. The very large microturbulent velocity in NGC6240 ($\xi \simeq 6$ km/s) is puzzling and may indicate that the red supergiants in this peculiar galaxy have very unusual properties.

6. Carbon depletion

As described in Sect. 4, the metallicities derived here are basically a measurement of the absolute Carbon abundance [C/H], and the values of [Fe/H] listed in Table 1 depend almost linearly on the assumed Carbon relative abundance [C/Fe]. However, this parameter influences the *shape* of the stellar spectra around 1.62 μm because the CO(6,3) band–head is flanked by OH bands, and their relative strengths depend on the C/O relative abundance or, equivalently, on the value of [C/Fe]. In the extreme case of very low Carbon relative abundances, in practice for [C/Fe]<–1, the CO(6,3) feature becomes much less evident, and the spectrum is dominated by OH bands. Such low values of [C/Fe] can be easily recognized, and excluded in our case, by simply comparing the depths of the strongest OH features at 1.622, 1625 μm, with the CO(6,3) band-head at 1.619 μm.

The variation of the OH/CO ratio with [C/Fe] can be estimated from Fig. 7a which compares our data for MC clusters with synthetic spectra computed adopting fiducial values for T_{eff} and log g, and using the microturbulent velocities derived above. For each value of [C/Fe] the metallicity is adjusted to match the short wavelength side of the CO(6,3) band–head.

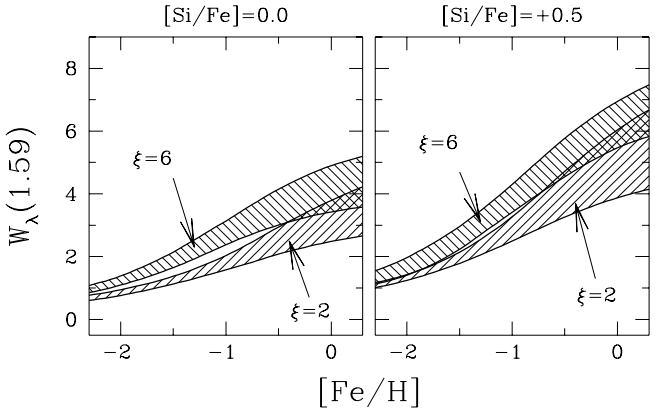

Fig. 8. Predicted variation of the Si–dominated index as a function of cluster metallicity for solar [Si/Fe] (left) and a Silicon enhancement of +0.5 dex (right hand panel). At each metallicity a large grid of models with different stellar parameters T_{eff} $\log g$ were computed (cf. Sect. 4), and the range of equivalent widths obtained is indicated by the shaded areas.

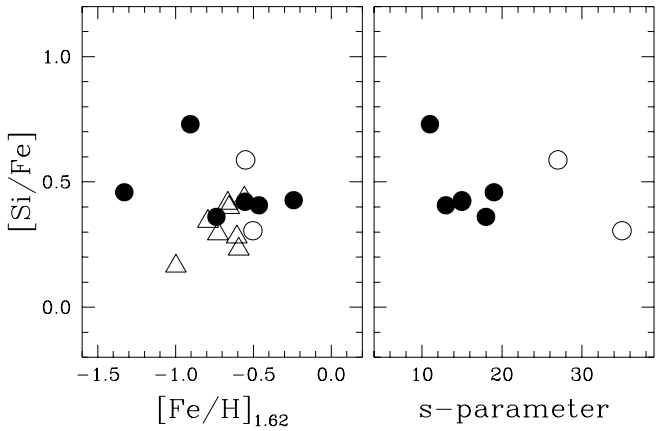

Fig. 9. [Si/Fe] is the Silicon relative abundance required to obtain the observed $W_\lambda(1.59)$ once [Fe/H]$_{1.62}$ is assumed. This parameter is plotted versus metallicity (left) and age parameter (right hand panel). Filled circles are MC clusters with $s<20$, open circles are older clusters with $s>20$ and open triangles are starburst galaxies.

The best fit value for the displayed objects is [C/Fe]$\sim$–0.3 and very similar values are also found for the other star clusters. Taking into account the not always excellent s/n of our spectra and the uncertainties on the adopted stellar parameters, we cautiously conclude that the data indicate –0.6<[C/Fe]<0.0, and are compatible with a standard C–depletion of –0.3 dex in the MC clusters.

A puzzling result is that, contrary to what found in MC clusters, the spectra of starburst galaxies do show significant variations of the relative strengths of the OH 1.625 and CO(6,3) 1.619 μm bands. The most extreme cases are the starbursters NGC4945 and NGC3256 whose spectra are displayed in Fig. 7b. While NGC4945 has OHλ1.625/COλ1.619$\simeq$0.7, the largest OH/CO ratio of all objects, the same ratio is only $\simeq$0.4 in NGC3256. This difference can be interpreted in two ways.

i) Variation of [C/Fe]. This is required if the red supergiants in the above galaxies have similar stellar temperatures and gravities. Assuming e.g. T_{eff}=3600 K and log g=0 yields [C/Fe]$\simeq$–0.6 and $\simeq$–0.0 in NGC4945 and NGC3256, respectively (cf. Fig. 7b).

ii) Variation of stellar parameters. The relative strengths of OH and CO lines also depend on T_{eff} and gravity. The effect of temperature is simply related to the fact that OH has a much lower dissociation potential than CO (4.4 and 11.1 eV, respectively), and therefore the OH/CO abundance ratio rapidly decreases with increasing T_{eff}. The effect of gravity is similar to that regulating the pressure dependence of atomic/ionic lines (cf. page 318 of Gray 1976). As g decreases, the total column density of the photosphere increases and so does N(CO) because most of the Carbon is in the form of CO, regardless on g. On the contrary, N(OH) remains roughly constant because OH/O$\ll$1 and therefore the OH relative abundance decreases at lower gravities. The effects of varying T_{eff} and log g can be visualized in Fig. 7b where synthetic spectra at different temperatures and gravities are compared with the data. These may indicate that the red supergiants in NGC4945 are cooler than the stars in NGC3256, but this cannot be easily reconciled with the fact that latter is more metallic than the former. An alternative possibility is that the stars in NGC4945 have significantly higher gravities than those in the MC clusters, and this would imply that the red supergiants in NGC4945 are less luminous, i.e. that the stellar population is older. The opposite reasoning holds for NGC3256 whose IR spectrum should be dominated by unusually luminous red hypergiants.

In short, the different OH/CO ratios found NGC4945 and NGC3256 could both imply that [C/Fe] varies significantly in these objects, or that the red supergiants in the two starburst galaxies have quite different average luminosities.

7. Silicon abundance

As already pointed out by OMO93 and OFFPO97, the 1.59 index is sensitive to the Silicon abundance but varies quite slowly with this parameter. This is evident in Fig. 8 which plots the predicted variation of the 1.59 index adopting the stellar parameters described in Sect. 4. Although $W_\lambda(1.59)$ cannot provide accurate measurements of [Fe/H], it can be however useful to roughly estimate the [Si/Fe] relative abundance. Silicon is an α element and it is expected to be enhanced as a consequence of primordial enrichment of the interstellar gas by type II supernovae if the star formation and collapse rates were relative fast, as possibly happened in the halo and bulge of our Galaxy (see e.g. Wheeler et al. 1989, Matteucci 1992).

The [Si/Fe] values needed to reproduce the metallicities inferred by the CO 1.62 line are listed in Table 1 and plotted in Fig. 9 as a function of metallicity and age. No obvious trend with either parameters is visible, and the average of [Si/Fe] is +0.45 and +0.32 for MC clusters and starburst galaxies, respectively. The Silicon enhancement for MC clusters is similar to that

found in old galactic globular clusters (OFFPO97) and therefore indicates a star formation history of the Clouds similar to that of our galaxy.

8. Conclusions

High quality IR spectra of young MC clusters have been used to derive information on the red supergiants dominating their 1.6 μm emission, and to obtain an independent estimate of their metallicities. A striking result is that the red supergiants appear to be much cooler than predicted by evolutionary models (Sect. 3), and this most probably reflects uncertainties in the treatment of the opacity and calibration of the mixing–length in the outermost layers of the stellar envelope.

Alike in old clusters, the metallicity can be readily estimated from the $W_\lambda(1.62)$ index which is here calibrated using synthetic stellar spectra (Sect. 4), and the method is also applied to eight starburst galaxies. The resulting values of [Fe/H] range between –1.3 for the SMC cluster NGC330 (in excellent agreement with previous estimates) to –0.2 for the LMC cluster NGC1994. Starburst galaxies have metallicities ranging between –1.0 (NGC6240) and –0.5 (NGC7552).

The metallicity scale presented here assumes a maximum temperature of 3600 K for the red supergiants. Since warmer stars require larger [Fe/H] to account for a given strength of the 1.62 feature (roughly +0.3 dex if T_{max}=4000 K and +0.7 dex if T_{max}=4300 K), the above metallicities could be more generally considered *lower limits* to the actual values.

The CO(2,0) and CO(6,3) band–heads are used to derive atmospheric microturbulent velocities. In MC clusters ξ is weakly correlated with the cluster metallicity, while starburst galaxies display largely scattered values. The most remarkable result is the large $\xi \simeq 6$ km/s value found in the low metallicity, peculiar galaxy NGC6240, and this may indicate that the red supergiants in this object have very unusual properties.

The data are also used to estimate Carbon depletion which influences the spectral shape around 1.62 μm (cf. Figs. 7a, 7b), and this opens interesting applications for deeper and higher resolution spectra with IR instruments of the next generation. Our spectra of MC clusters are compatible with a 'standard' value of [C/Fe]$\simeq$–0.3. Interestingly, evidences of significant variations of [C/Fe] are found in some starburst galaxies, the most extreme cases being NGC3256 and NGC4945 whose spectra require [C/Fe]$\simeq$–0.0 and –0.6, respectively. However, the data can also be reconciled with normal C–depletions if the red supergiants in these galaxies have very different, and somewhat unusual temperatures and/or surface gravities.

Finally, the Silicon relative abundance is roughly estimated from the 1.59 feature. The value of [Si/Fe] in MC clusters is about +0.5 and similar to that found in old clusters of our galaxy, this indicates a primordial enrichment of Silicon in the interstellar medium of the Clouds due to type II supernovae.

Acknowledgements. We are grateful to A. Bressan and O. Straniero for elucidating discussions on evolutionary models. We thank G. Wiedemann, the referee, for comments which helped improving the quality of the paper. We also thank K. Hinkle for providing us with unpublished high resolution 1.6 μm spectra of α-Ori, which we used to verify the accuracy of our synthetic spectral spectra.

References

Barbuy B., Spite M., Spite F., Milone A., 1991, A&A 247, 15
Bertelli. G., Bressan A., Chiosi C., Fagotto F., Nasi E., 1994, A&AS 106, 275 (B94)
Castellani V., Chieffi A., Straniero O., 1990, ApJS 74, 463
Charbonnel C., Meynet G., Maeder A., Schaller G., Schaerer D., 1993, A&AS 101, 415
Chieffi A., Straniero O., Salaris M., 1995, ApJL 445, L39
Chiosi C., Bertelli G., Bressan A., Nasi E., 1986, A&A 165, 84
Chiosi C., Vallenari A., Bressan A., Deng L., Ortolani S., 1995, A&A 293, 710
Elson R.A.W., Fall S.M., 1985, ApJ 299, 211
Elson R.A.W., Fall S.M., 1988, AJ 96, 1383
Ferraro F.R., Fusi Pecci F., Testa V. et al., 1995, MNRAS 272, 391
Gonzalez–Delgado R.M., Perez E., Diaz A.I. et al., 1995, ApJ 439, 604
Gray D.F, 1976, *The Observation and Analysis of Stellar Photospheres*, Wiley-Interscience Pub., New York
Gredel R., Weilenman U., 1992, The Messenger 70, 62
Maeder A., Conti P.S., 1994, ARA&A 32, 227
Marconi G., Matteucci F., Tosi M., 1994, MNRAS 270, 35
Matteucci F., 1992, Mem. S.A.It. 63, 301
McGaugh S.S., 1991, ApJ 380, 140
Meliani M.T., Barbuy B., Richtler T., 1994, A&A 290, 753
Meliani M.T., Barbuy B., Perrin M.N., 1995, A&A 300, 349
Moorwood A.F.M., Moneti A., Gredel R., 1991, The Messenger 63, 77
Oliva E., Origlia L., 1992, A&A 280, 536
Oliva E., Origlia L., Kotilainen J.K., Moorwood A.F.M., 1995, A&A 301, 55 (OOKM95)
Origlia L., Moorwood A.F.M., Oliva E., 1993, A&A 280, 536 (OMO93)
Origlia L., Ferraro F.R., Fusi Pecci F., Oliva E., 1997, A&A 321, 859 (OFFPO97)
Renzini A., Buzzoni A., 1986, *Spectral Evolution of Galaxies*, eds. C. Chiosi & A. Renzini, p. 195
Richtler T., Nelles B., 1983, A&A 119, 75
Ritossa C., 1996, MNRAS 281, 970
Sagar R., Pandey A.K., 1989, A&AS 79, 407
Stasinska G., Leitherer C., 1996, ApJS 107, 661
Storchi–Bergmann T., Calzetti D., Kinney A.L., 1994, ApJ 429, 572
Wheeler J.C., Sneden C., Truran J.W. Jr., 1989, ARA&A 27, 279
Worthey G., 1994, ApJS 95, 107

This article was processed by the author using Springer-Verlag LaTeX A&A style file *L-AA* version 3.